Arousal fluctuations govern oscillatory transitions between dominant gamma and alpha occipital activity during eyes open/closed conditions

Axel Hutt, Jérémie Lefebvre

Brain Topography manuscript No.
(will be inserted by the editor)

Arousal fluctuations govern oscillatory transitions between dominant γ and α occipital activity during eyes open/closed conditions

Axel Hutt · Jérémie lefebvre

Received: date / Accepted: date

Abstract Arousal results in widespread activation of brain areas to increase their response in task and behavior relevant ways. Mediated by the Ascending Reticular Arousal System (ARAS), arousal-dependent inputs interact with neural circuitry to shape their dynamics. In the occipital cortex, such inputs may trigger shifts between dominant oscillations, where α activity is replaced by γ activity, or vice versa. A salient example of this are spectral power alternations observed while eyes are opened and/or closed. These transitions closely follow fluctuations in arousal, suggesting a common origin.To better understand the mechanisms at play, we developed and analyzed a computational model composed of two modules: a thalamocortical feedback circuit coupled with a superficial cortical network. Upon activation by noise-like inputs originating from the ARAS, our model is able to demonstrate that noise-driven nonlinear interactions mediate transitions in dominant peak frequency, resulting in the simultaneous suppression of α limit cycle activity and the emergence of γ oscillations through coherence resonance. Reduction in input provoked the reverse effect - leading to anticorrelated transitions between α and γ power. Taken together, these results shed a new light on how arousal shapes oscillatory brain activity.

A. Hutt
Team MIMESIS, INRIA Nancy - Grand Est, France
E-mail: axel.hutt@inria.fr

J. Lefebvre
Department of Biology, University of Ottawa, Ottawa, ON K1N 6N5, Canada
Krembil Research Institute, University Health Network, Toronto, ON M5T 0S8, Canada
Department of Mathematics, University of Toronto, Toronto, ON M5S 2E4, Canada
E-mail: Jeremie.Lefebvre@uottawa.ca

Keywords coherence resonance · ascending reticular arousal system · cortico-thalamic feedback

1 Introduction

Arousal is a mechanism in vertebrates that characterizes simultaneous, widespread and behaviorally relevant activation of multiple brain areas. Signatures of arousal in animals include enhanced responsiveness to sensory stimuli, increased motor recruitment, as well amplified emotional responses in humans (Quinkert et al. 2011). Arousal is mediated through the selective activation of the Ascending Reticular Arousal System (ARAS) (Brown et al. 2012; Edlow et al. 2012; Fuller et al. 2011; Koval'zon 2016; Moruzzi and Magoun 1949; Steriade 1996). The ARAS plays an important role in regulating the different stages of wakefulness, the endocrine and autonomous nervous system and regulates the cardiovascular system by modulating the overall excitability level in the brain. To do this, ARAS projections innervate directly and/or indirectly various sub-cortical and cortical brain regions (Brown, Lydic, and Schiff 2010; Edlow et al. 2012; Fuller et al. 2011), such as the thalamus (Schiff 2008; Steriade 1996) and the cortex (Franks 2008; Lakatos et al. 2004; McNally et al. 2020). It is thus no surprise that through these widespread projections, the ARAS influences cognitive processes and behaviour significantly. Prominent examples of arousal-driven effects include increased attention (Coull 201998; Lakatos et al. 2004), sleep (Richter, Woods, and Schier 2014; Steriade, McCormick, and Sejnowski 1993) as well as anaesthetic-induced loss of consciousness (Brown, Lydic, and Schiff 2010; Franks 2008; Hutt 2011). As a corollary, arousal - and thus the ARAS - impact significantly oscillatory brain activity.

A salient and still puzzling phenomenon is the change in occipital α rhythmic activity (8Hz-12Hz) observed whenever subjects and animals open and/or close their eyes and overt behavior. This phenomenon, historically referred to event related desynchronization and desynchronization (ERD/ERS), has been repetitively shown to track changes in cortical activation states (Pfurtscheller and Silva 1999). The origin of the so-called Berger rhythm (Adrian and Matthews 1935; Berger 1935) as well as the mechanisms responsible of task-related α power fluctuations is still under active debate. Broadly speaking, there are two main hypotheses for the generation of this salient rhythmic phenomenon. Historically, first claims that the occipital cortex generates the α rhythm is supported by more recent experimental evidence (Bollimunta et al. 2008), as well as by behavioural studies pointing out the importance of the $\alpha-$rhythm in visual attention (Thut et al. 2006). Building on these observations, another main hypothesis states that $\alpha-$ activity has a thalamic origin (Hughes and Crunelli 2005; Vijayan and Kopell 2012), while recent experiment studies further suggest that these oscillations propagate in the form of travelling waves to drive the thalamus (Halgren et al. 2019). To this end, an emergent view in which cortico-thalamic feedback - involving both occipital cortex and thalamic structures - generates the $\alpha-$ rhythm has received strong support from both experimental and theoretical studies (Bollimunta et al. 2011; Hashemi, Hutt, and Sleigh 2015; Hutt 2019; Hutt et al. 2018; Sleigh et al. 2011). Given significant fluctuations in α-power during arousal and/or visual attention, it however remains unclear how the ARAS interact with cortico-thalamic feedback projections to mediate observed changes in occipital oscillatory activity.

Activation of the visual system , e.g. by opening/ closing the eyes or by attention, does not only alter occipital $\alpha-$rhythms but also cortical $\gamma-$ activity within the same regions (Geller et al. 2014), cf. Fig. 1(A). Interestingly, such focal changes in α and γ power are oftentimes anti-correlated with one another: increases in $\alpha-$ activity follows concomitant decreases in γ power, and vice versa. Geller et al. (2014) have found experimentally strong occipital $\gamma-$ activity and weak $\alpha-$ activity in ECog-data when the subject has open eyes, whereas the inverse occurs with closed eyes. This anti-correlation, characterized by focal shifts in dominant oscillatory frequency in occipital regions suggests that both these rhythms are regulated by a common, arousal-dependent input. Specifically, recalling the arousal- dependent $\alpha-$ activity, we raise the question whether fluctuations in $\gamma-$ activity may also result from changes in arousal through an interference with the cortico-thalamic feedback loop. In support of this hypothesis, it is well-known that arousal induces cortical $\gamma-$rhythms (Kim et al. 2015; Lakatos et al. 2004; McNally et al. 2020; Steriade et al. 1991b) and tunes synchronisation in the visual cortex (Fries et al. 2001; Lee et al. 2003; Munk et al. 1996). Recently, Pisarchik et al. (2019) have taken up the idea of *coherence resonance* (Gang et al. 1993; Longtin 1997; Pikovsky and Kurths 1997) and have proposed that "neural circuits adapt their [intrinsic] noise level according to cognitive demand in order to increase signal-to-noise ratio". By noise, we refer here to statistically uncorrelated fluctuations stemming from elevated neural spiking activity. This is in line with recent results of Hakim, Shamardani, and Adesnik (2018) revealing $\gamma-$band coherence in the visual cortex by non-oscillatory stimulation.

Recently, Lefebvre, Hutt, and Frohlich (2017) have proposed that fluctuations in $\alpha-$ power may be induced by ARAS-driven noisy inputs to the thalamus, interfering with the cortico-thalamic feedback loop. In the present study, we built on those results and developed a feedback model that generates both α and γ oscillatory activity and further depends on ARAS-mediated stochastic drive. We have enhanced our model by including not only cortio-thalamic feedback but also distinct cortical layers to better capture laminar cortical responses to thalamic and ARAS inputs. Since the ARAS projects both to the cortex and the thalamus (cf. Fig. 2), we hypothesized that ARAS-mediated inputs would engage cortico-thalamic feedback loop to support changes in oscillatory neural activity across both cortical and thalamic populations. We assumed that this tuning mediated by ARAS - and hence arousal - occurs when eyes are opening/closing, through increase in visual attention (Bollimunta et al. 2011) or, alternatively, during drowsiness or REM-sleep, as seen experimentally (Cantero et al. 1999). Since the ARAS projects to supragranular cortical layers (Koval'zon 2016), we follow the line of thought of Pisarchik et al. (2019) and hypothesise that cortical $\gamma-$ activity is noise-induced and the ARAS contributes to this cortical noise. Consequently, the cortical dynamics may obey a coherence resonance mechanism - this is what we explore here. Figure 1(B) presents the spectral power distribution of simulated EEG in the course of time and one observes a qualitative agreement with the alternating dominance of $\alpha-$ and $\gamma-$rhythms.

The subsequent sections introduces the ARAS as a regulator of input to the thalamus and cortex as well as the cortico-thalamic feedback and intracortical coherence resonance model. Both these models combine to describe $\alpha-$ and $\gamma-$ activity under *eyes open* and *eyes closed* conditions. The Results section presents the

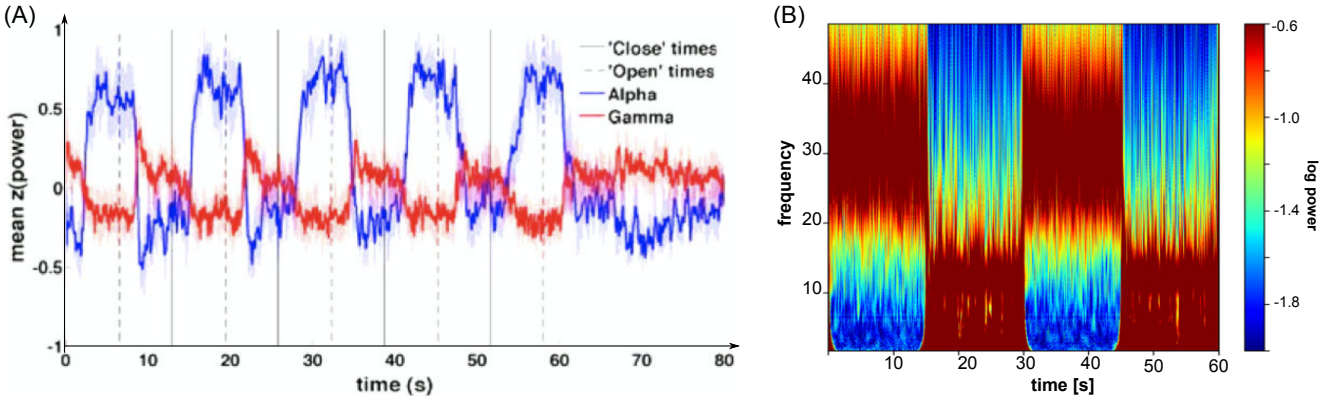

Fig. 1 Experimental electrocorticogram (ECog) in the occipital cortex and model simulations for alternating *eyes open* and *eyes closed* conditions. (A) The plot shows transformed power in the $\alpha-$ and γ-frequency band, that alternates in the course of time. Modified from Figure 2 in (Geller et al. 2014) with permission. (B) Time-frequency log-power plot of simulated EEG-data showing alternating power in the γ- $(25-40\text{Hz})$ and $\alpha-(8-14\text{Hz})$ frequency band. See the Method section for more details.

gained results and explains the dynamical mechanisms in detail. The Discussion summarizes the results and embeds them into current literature.

2 Methods

2.1 The relationship between ARAS activation and intrinsic noise

The ARAS is known to drive the brain and sets its level of excitability. For instance, anaesthetics diminish thalamic input to the cortex, reduces cortical and thalamic firing activity and induce sedation and loss of consciousness at larger concentration. In the ARAS, brain stem sub-structures play an important role and notably contribute to the cortico-thalamic feedback loop and the excitation level in the cerebral cortex. Specifically, there is experimental evidence that the brain stem contributes to the occipital and parietal α-rhythm (Brown et al. 2012) and indirectly via the ARAS the cortical γ-rhythms (Kim et al. 2015; Lakatos et al. 2004; McNally et al. 2020). Recently, a modelling study has proposed that ARAS activity contributes primarily to the generation of frontal EEG $\alpha-$ activity under propofol anaesthesia (Hutt et al. 2018). This study assumes that the ARAS drives the cortical and thalamic structures by uncorrelated noise.

The ARAS is not a *diffusive* system as assumed after the ground-breaking work of Moruzzi and Magoun (1949), but comprises several sub-arousal systems (Koval'zon 2013, 2016; Richter, Woods, and Schier 2014). In order to understand the role of the ARAS in shaping brain dynamics, a first approximation of its rather complex activity may nonetheless provide insights. To this end, we consider ARAS-mediated input as additive noise, interacting with both the cortico-thalamic feedback loop and the cortex, with arousal-dependent statistics (i.e. mean and variance). Such noise is assumed to mimic uncorrelated synaptic bombardment resulting from spiking activity projecting from the ARAS neurons. Consequently, strong and weak arousal in the ARAS reflect high and low intrinsic noise intensity, respectively. Inspired by experimental observations and the relation between arousal and intrinsic noise activation by the ARAS, we hypothesise that for high arousal condition (e.g. eyes open), strong $\gamma-$ and weak $\alpha-$ activity are characterized by high intrinsic noise level. In contrast, weak γ- and strong α-activity - characterizing low arousal (e.g. eyes closed) would reflect reduced intrinsic noise level.

To model the effect of arousal and ARAS inputs, we introduce the arousal state function $e(t)$ that relates the intrinsic noise level in both cortical and thalamic populations with the state of arousal i.e.

$$e(t) = \frac{2}{\pi}\,\text{atan}\left(\frac{\sin(2\pi p t/T)}{s}\right) \quad , \quad 0 \le t \le T \tag{1}$$

with $0 < e(t) < 1$ and the scaling factor $s = 0.05$, the number of periods $p = 20$ and the total simulation time $T = 1.2pT_{\text{segment}}$. The interval T_{segment} is the duration of an arousal state sequence *eyes open - eyes closed*. If $e(t)$ is maximum at $e \approx 1$, then eyes are open and the intrinsic noise level is maximum. The minimum value $e \approx 0$ reflects closed eyes and the intrinsic noise level is minimum. The power spectrum of the neural activity computed in each of the two segments should have a frequency resolution df that dictates $T_{\text{segment}} = 2/f_s df$ with the sampling rate f_s. Figure 3(A) shows the arousal state function $e(t)$ where we define the condition *eyes open* for $e(t) \ge 0.5$ and *eyes closed* for $e(t) < 0.5$.

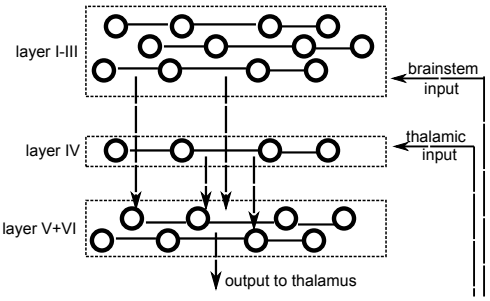

Fig. 2 Schematic of cortical layers and afferent/efferent connections projecting to different populations.

Taken together, the intrinsic noise intensity across both cortical and sub-cortical populations is given by

$$D(t) = D_{\min} + (D_{\max} - D_{\min})e(t) \tag{2}$$

with maximum and minimum noise level $D_{\max}$ and $D_{\min}$. The choice of $D_{\max}$ and $D_{\min}$ is different for the model type and neuron types introduced in the subsequent section 2.2.

2.2 The network model

The present work aims to characterize changes between $\alpha-$ and γ-power in visual cortex while arousal level is changing in subjects with open and/or closed eyes. There is strong evidence that resting α-rhythms originate from the feedback connection between the cortex and thalamic structures, while $\gamma-$rhythms emerge from local intra-cortical connections. By virtue of the layer physiology in the cerebral cortex, cf. Fig. 2, a network model in layers I-III describes the emerging $\gamma-$activity while a cortico-thalamic feedback network including input layer IV and output layers V and VI models describes $\alpha-$activity.

Cortical module: microscopic multi-layers network of excitatory and inhibitory cortical neurons

The model for layer I-III (Hutt et al. 2020)

$$\begin{aligned}
\frac{1}{\alpha_{ic}}\frac{dV_n^e}{dt} &= -V_n^e(t) + H_0 \sum_{m=1}^{N} K_{nm}^{\text{self}} H[V_m^e(t)] \\
&\quad - \sum_{m=1}^{N} K_{nm}^{\text{inter}} H[V_m^i(t)] + I_e^{ic} + \xi_n^{\text{ic}}(t) \\
\frac{1}{\beta_{ic}}\frac{dV_n^i}{dt} &= -V_n^i(t) - \sum_{m=1}^{N} K_{nm}^{\text{self}} H[V_m^i(t)] \\
&\quad + H_0 \sum_{m=1}^{N} K_{nm}^{\text{inter}} H[V_n^e(t)] + I_i^{ic} + \eta_n^{\text{ic}}(t)
\end{aligned} \tag{3}$$

with $n = 1, \ldots, N$ assumes excitatory and inhibitory synapses with respective dendritic currents $V_n^e(t)$ and $V_n^i(t)$ at network node n and time t. The network is populated by interconnected excitatory and inhibitory neurons located at each node, whose synaptic properties are identical in both cell types. Each neuron at a node is a McCullogh-Pitts neuron with firing rate step function $H[V] = 0$ for $V < 0$ and $H[V] = 1$ for $V \geq 0$ and the relative maximum firing rate of both cell types is given by the scalar factor H_0. The connection matrix K_{nm}^{self} denotes the intra-population connection weights, i.e. between excitatory neurons and between inhibitory neurons, and the matrix K_{nm}^{inter} reflects the connections between excitatory and inhibitory neurons.
External fluctuating input stimulates each cell with constant mean I_e^{ic}, I_i^{ic} and random fluctuations $\xi_n^{\text{ic}}(t)$, $\eta_n^{\text{ic}}(t)$. We assume that the noise ξ_n^{ic}, η_n^{ic} has zero mean and variances D_e^{ct}, D_i^{ct} with

$$\langle \xi_n^{\text{ic}}(t)\xi_m^{\text{ic}}(\tau)\rangle = D_e^{\text{ct}} \ , \ \langle \eta_n^{\text{ic}}(t)\eta_m^{\text{ic}}(\tau)\rangle = D_i^{\text{ct}}.$$

These random fluctuations originate from intrinsic noise processes and ARAS via the brain stem, cf. Fig. 2. We point out that the noise variances may depend on the experimental condition, cf. Eq. (2). The present work considers primarily the mean-field dynamics in this network (cf. section 2.3) and we refer the reader to (Hutt et al. 2020) for more details on the single neuron model.

Thalamo-cortical module: microscopic network of interacting cortical and subcortical populations

We further introduce a hybrid model that describes network dynamics in cortical layers V and VI including the cortico-thalamic feedback and input from cortical layers I-III. The network of N nodes obeys the following evolution equations

$$\begin{aligned}
\frac{1}{\alpha_{\text{ct}}}\frac{du_n^e}{dt} &= -u_n^e(t) + bA_n^e(t) + S_n^{ee}(t-\tau) + S_n^{ei}(t-\tau) \\
&\quad + I_e^{ct} + \sum_{m=1}^{N} C_{nm} V_m^e(t) + \xi_n^{\text{ct}}(t) \\
\frac{1}{\beta_{\text{ct}}}\frac{du_n^i}{dt} &= -u_n^i(t) + bA_n^i(t) + S_n^{ie}(t-\tau) + S^{ii}(t-\tau) \\
&\quad + I_i^{ct} + \eta_n^{\text{ct}}(t) \\
\frac{1}{a}\frac{dA_n^e}{dt} &= -A_n^e(t) + u_n^e(t) \\
\frac{1}{a}\frac{dA_n^i}{dt} &= -A_n^i(t) + u_n^i(t) \ .
\end{aligned} \tag{4}$$

with $n = 1, \ldots, N$ and where u_n^e and u_n^i are the effective excitatory and inhibitory potentials generated of

excitatory and inhibitory neurons, respectively, at network node n. The delayed interaction with delay time τ represents an effective propagation time from layers V and VI to thalamic structures and back to the cortex via input layer IV. In the cerebral cortex, layers V and VI receive excitatory input from cortical layers I-III which enter our model by the coupling matrix $\mathbf{C}$. The neuron's dynamics further consider synaptic adaption described by the currents $A_n^e,\ A_n^i$, cf. (Hutt et al. 2018). The parameters $\alpha_{\rm ct},\ \beta_{\rm ct}$ and a are temporal membrane rates of the respective cell type and the temporal adaption rate. In addition, the neurons receive synaptic input expressed by

$$S_n^{kl}(t) = \frac{1}{N}\sum_{m=1}^{N} W_{nm}^{kl} E_m^{kl}(t) \quad , \quad k,l = \{e,i\}$$

with the synaptic weights W_{nm}^{kl} of connection between node n and m and the synaptic response function $E_m^{kl}(t)$ obeying

$$\tau^l \frac{dE_m^{kl}(t)}{dt} = -E_m^{kl}(t) + X_m^k(t) \ .$$

Here τ^l denotes the time scale of synapses of type $l = \{e,i\}$. The spike train $X_m^k(t)$ is generated by a non-homogeneous Poisson process for a neuron of type k at node m with rate $f(u_m^k)$.
External constant input $I_e^{\rm ct},\ I_i^{\rm ct}$ and fluctuating input $\xi_n^{\rm ct},\ \eta_n^{\rm ct}$ stimulate the neurons. The fluctuating inputs are independent, identically distributed Gaussian processes with zero mean and they share the variance $D_o^{\rm ct}$, i.e.

$$\langle \xi_n^{\rm ct}(t)\xi_m^{\rm ct}(\tau)\rangle = D_o^{\rm ct} \ , \ \langle \eta_n^{\rm ct}(t)\eta_m^{\rm ct}(\tau)\rangle = D_o^{\rm ct} \ .$$

These random fluctuations originate from intrinsic noise processes in the single neurons and the ARAS stimulating the thalamus and their variances may depend on the experimental condition, cf. Eq. (2). For more details, we refer the reader to (Hutt et al. 2018). The present work considers primarily the mean-field dynamics in this network that is described in more detail in section 2.3.

2.3 Mesoscopic dynamics: combining cortical and cortico-thalamic modules

Experimental data gathered at larger spatial scales, such as EEG measured on the scalp or ECog observed on the top of the cortex, map the collective activity of very large population of neurons. To this end, mean-field descriptions of microscopic modules (both intra cortical and thalamo-cortical) enables a comparison between simulated and observed data, as well and derive deeper insights into underlying dynamical mechanisms at play in arousal-mediated oscillatory transitions.

The mean-field model derived from the intra-cortical module equations (3) reads (Hutt et al. 2020)

$$\begin{aligned}\frac{1}{\alpha_{ic}}\frac{dV_e}{dt} &= -V_e(t) + EK_{\rm self}S_e^{\rm ic}[V_e(t)] - K_{\rm inter}S_i^{\rm ic}[V_i(t)] \\ &\quad + I_e^{ic} + \xi_{\rm ic}(t) \\ \frac{1}{\beta_{ic}}\frac{dV_i}{dt} &= -V_i(t) - K_{\rm self}S_i^{\rm ic}[V_i(t)] + EK_{\rm inter}S_e^{\rm ic}[V_e(t)] \\ &\quad + I_i^{ic} \ .\end{aligned} \tag{5}$$

The set of equations describe the dynamics of the mean time-dependent dendritic currents

$$V_e(t) = \frac{1}{N}\sum_{n=1}^{n} V_n^e(t) \ , \ V_i(t) = \frac{1}{N}\sum_{n=1}^{n} V_n^i(t) \ .$$

Excitatory and inhibitory neurons excite and inhibit themselves with mean weight $F_{\rm self}$, respectively. Moreover, excitatory (inhibitory) neurons excite (inhibit) inhibitory (excitatory) neurons with weight $K_{\rm inter}$. The parameter E weights the excitation relative the inhibition. The model is reminescent of the celebrated Amari neural population model (Amari 1977). In the stochastic mean-field description presented here, it is important to distinguish microscopic and macroscopic fluctuations. The model (5) describes the temporal evolution of the mean of a nonlinearly coupled network subjected to additive microscopic noises $\{\xi_n^{\rm ic}\},\ \{\eta_n^{\rm ic}\}$ at each network node, cf. Eqs. (3). These random fluctuations at the microscopic level interact with the network nonlinear transfer function, resulting in a linearized effective non-linear structure. This effect has been shown in detail in several previous studies (Herrmann et al. 2016; Hutt, Mierau, and Lefebvre 2016; Hutt et al. 2018, 2020; Lefebvre, Hutt, and Frohlich 2017; Lefebvre et al. 2015; Rich et al. 2020). Roughly speaking, the stronger the noise, the more flat the transfer function. The model (5) for vanishing macroscopic fluctuations $\xi_{\rm ic} = 0$ would assume that the microscopic additive noise is identically independent Gaussian distributed with constant network mean and variance. If, however, the network mean and variance fluctuate randomly themselves over time, then the mean-field dynamics itself is stochastic (Hutt et al. 2020). Since it is realistic to assume a fluctuating network mean and variance, it is necessary to add the term $\xi_{\rm ic} \neq 0$. Hence $\xi_{\rm ic}$ denotes small random macroscopic input originating from intrinsic network fluctuations and possibly macroscopic external input from other brain areas. We assume i.i.d. Gaussian distributed fluctuations with $\langle \xi_{\rm ic}\rangle = 0$, $\langle \xi_{\rm ic}(t)\xi_{\rm ic}(t')\rangle = D_{\rm ic}$ with the

macroscopic noise variances $D_{\rm ic}$.

The mean-field representation of the cortico-thalamic microscopic module equations (4) reads

$$\begin{aligned}
\frac{1}{\alpha_{\rm ct}}\frac{dU_e}{dt} &= -U_e(t) + bA_e(t) + K_{ee}S_e^{\rm ct}[U_e(t-\tau)] \\
&\quad - K_{ei}S_i^{\rm ct}[U_i(t)] + cV_E(t) + I_e^{\rm ct} + \xi_{\rm ct}(t) \\
\frac{1}{\beta_{\rm ct}}\frac{dU_i}{dt} &= -U_i(t) + bA_i(t) + K_{ie}S_e^{\rm ct}[U_e(t-\tau)] \\
&\quad - K_{ii}S_i^{\rm ct}[U_i(t-\tau)] + I_i^{\rm ct} \\
\frac{1}{a}\frac{dA_e}{dt} &= -A_e(t) + U_e(t) \\
\frac{1}{a}\frac{dA_i}{dt} &= -A_i(t) + U_i(t)
\end{aligned} \tag{6}$$

with the mean time-dependent potentials

$$U_{e,i}(t) = \frac{1}{N}\sum_{n=1}^{n} u_n^{e,i}(t)\ ,\ A_{e,i}(t) = \frac{1}{N}\sum_{n=1}^{n} A_n^{e,i}(t)\ .$$

located in cortical layers V-VI and the synaptic mean adaption variables $A_e(t),\ A_i(t)$. In contrast to Eq. (5), this model corresponds to a set of hybrid Wilson-Cowan equations (Wilson and Cowan 1972). Equation (6) is an effective reduced model of the cortico-thalamic feedback loop with net delay τ that receives input from layers I-III with coupling constant c. The external input $\xi_{\rm ct}$ represents macroscopic i.i.d. Gaussian random fluctuations originating from intrinsic fluctuations and external input from other brain areas with $\langle\xi_{\rm ct}\rangle = 0$, $\langle\xi_{\rm ct}(t)\langle\xi_{\rm ct}(t')\rangle = D_{\rm ct}\delta(t-t')$ with the macroscopic noise variances $D_{\rm ct}$.

The effective mean-field transfer functions in both models are defined by

$$S_n^m(x) = \frac{1}{2}\left(1 + \mathrm{erf}\left(\frac{x-\Theta^m}{\sqrt{2\sigma_n^m}}\right)\right)$$

with $n = \{e,i\},\ m = \{\mathrm{ct},\mathrm{ic}\}$, the mean firing threshold Θ_m and the steepness rate σ_n^m. They represent the population rate of incoming spikes relative to a maximum firing rate and thus reflect a firing probability (Hutt and Buhry 2014). We point out that the transfer functions result from the microscopic properties of the network, like the firing rate function of individual neurons (Hutt and Buhry 2014) and the intrinsic microscopic noise level (Hutt et al. 2020). In more detail, the steepness rates of both neuron types $\sigma_{e,i}^m$ depend on the intrinsic noise levels $D_{e,i}^m$, cf. section 2.2, by

$$\begin{aligned}
\sigma_e^{\rm ic} &= D_e^{\rm ic}(t) \\
\sigma_i^{\rm ic} &= D_i^{\rm ic} = \mathrm{const} \\
\sigma_e^{\rm ct} &= D_o^{\rm ct}(t)\sqrt{2}\left(\frac{{A_+^e}^2}{2\lambda_+^e} + \frac{2A_+^eA_-^e}{\lambda_+^e+\lambda_-^e} + \frac{{A_-^e}^2}{2\lambda_-^e}\right) \\
\sigma_i^{\rm ct} &= D_o^{\rm ct}(t)\sqrt{2}\left(\frac{{A_+^i}^2}{2\lambda_+^e} + \frac{2A_+^iA_-^i}{\lambda_+^e+\lambda_-^e} + \frac{{A_-^i}^2}{2\lambda_-^e}\right)
\end{aligned}$$

with

$$\begin{aligned}
\lambda_\pm^e &= \frac{1}{2}\left(\alpha_{\rm ct}a \mp \sqrt{(\alpha_{\rm ct}-a)^2 + 4b\alpha_{\rm ct}a}\right) \\
\lambda_\pm^i &= \frac{1}{2}\left(\beta_{\rm ct}a \mp \sqrt{(\beta_{\rm ct}-a)^2 + 4b\beta_{\rm ct}a}\right) \\
A_+^e &= \sqrt{2\pi}\frac{a-\lambda_+^e}{\lambda_-^e-\lambda_+^e} \\
A_-^e &= -\sqrt{2\pi}\frac{a-\lambda_-^e}{\lambda_-^e-\lambda_+^e} \\
A_+^i &= \sqrt{2\pi}\frac{a-\lambda_+^i}{\lambda_-^i-\lambda_+^i} \\
A_-^i &= -\sqrt{2\pi}\frac{a-\lambda_-^i}{\lambda_-^i-\lambda_+^i}\ .
\end{aligned}$$

The noise variances $D_e^{\rm ic}(t),\ D_o^{\rm ct}(t)$ depend on the arousal level as per Eq. (2) whereas the noise variance in inhibitory intracortical neurons $D_i^{\rm ic}$ remains constant.

The nonlinear dynamics of both model systems (5, 6) may be explained by the dynamic topology about their equilibria. Neglecting the additive noise $\xi_{\rm ic}(t),\ \xi_{\rm ct}(t)$, the equilibria are defined by $dV_e/dt = dV_i/dt = dU_e/dt = dU_i/dt = dA_e/dt = dA_i/dt = 0$ and their stability reads off the Jacobian eigenvalue spectrum. This spectrum permits to classify the equilibria and indicates the shape of the expected power spectrum of the system signal close to the equilibrium in the presence of weak noise. For instance, if the eigenvalue spectrum of an equilibrium has real eigenvalues only, then the linear power spectrum has a maximum at zero frequency only. A spectral peak at non-zero frequency may be present if the eigenvalue spectrum has complex eigenvalues and the frequency of the power peak may be close to the imaginary part of the complex eigenvalues (Hutt 2013). Such an activity is called a *quasi-cycle*. If, in addition, this stable focus is generated and destroyed by increasing the system's noise, then one calls this effect *coherence resonance*. This is found in the intracortical model as shown in the Results section.

2.4 Simulated EEG

To gain synthetic EEG data, we have integrated numerically Eqs. (5,6) with an Euler-Maruyama scheme (Buck-

Table 1 Parameter set of model (5) and (6) to generate results shown in Fig. 3 and 4.

parameter	description	value
α_{ic}	exc. synaptic rate	200 Hz
β_{ic}	inh. synaptic rate	50 Hz
K_{self}	synaptic weight	3.7
K_{inter}	synaptic weight	3.9
I_e^{ic}	constant input	1.1
K_i^{ic}	constant input	0.4
D_{ic}	noise variance	10^{-5}
α_{ct}	exc. membrane rate	50 Hz
β_{ct}	inh. membrane rate	100 Hz
a	adaption rate	5 Hz
b	adaption coupling	0.5
K_{ee}	coupling weight	2.21
K_{ei}	coupling weight	3.46
K_{ie}	coupling weight	4.58
K_{ii}	coupling weight	1.69
I_e^{ct}	constant input	0.1
I_i^{ct}	constant input	0.0
D_{ct}	macr. noise variance	10^{-7}
τ	time delay	14 ms
Θ^{ct}	firing threshold	0.1
Θ^{it}	firing threshold	0.0
D_i^{it}	micr. noise variance	0.5
$D_{\mathrm{min}}^{\mathrm{ic}}$	micr. noise variance	0.1
$D_{\mathrm{max}}^{\mathrm{ic}}$	micr. noise variance	0.8
$D_{o,\mathrm{min}}^{\mathrm{ct}}$	micr. noise variance	1.2
$D_{o,\mathrm{max}}^{\mathrm{ct}}$	micr. noise variance	1.4
w	weight in EEG signal	0.5
E	weight of excitation to inhibition	1.7
c	weight of ic model in ct	0.01

war and Winkler 2007) with integration time step $\Delta t = 5 \cdot 10^{-4}$ and the parameters from Table 1.

Experimental multi-array studies in visual areas V2 and V4 (Bollimunta et al. 2008) have indicated that layers V+VI are the most likely occipital α-generators. Since our effective cortico-thalamic feedback model (6) describes the mean potentials in this layer and excitatory neurons are supposed to dominate EEG activity, we assume that the EEG depends strongly on $U_e(t)$ in Eqs. (6). Moreover, EEG or ECog may also capture strong activity in layers I-III modelled as $V_e(t)$. However, since it is difficult to quantify the respective contributions of both possible EEG/ECOG sources, i.e. the activity in layers I-III and layers V+VI, we assume a relative weight w between both signals and define the synthetic observed EEG as

$$\mathrm{EEG}(t) = (1-w)V_e(t) + wU_e(t). \tag{7}$$

Experimental EEG-signals are sampled with a sampling rate f_s, and as such, we downsampled EEG(t) to $f_s = 500$Hz.

To investigate possible alternations of power in the $\alpha-$ and γ-frequency band mediated by arousal, we band pass-filtered the EEG signal accordingly. To this end,

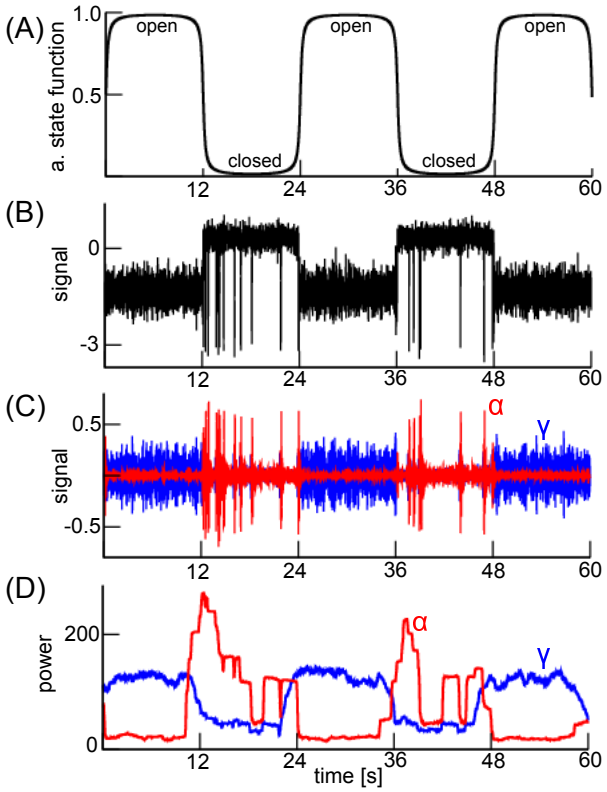

Fig. 3 Simulated EEG for alternations between *eyes closed* and *eyes open*. (A) Arousal state function $e(t)$ taken from Eq. (1). (B) simulated EEG signal (7). (C) Bandpass-filtered EEG signal showing $\alpha-$activity (red) and $\gamma-$activity (blue). (D) Instantaneous power of the bandpass-filtered EEG (8)
.

we employ a Butterworth-filter of 4th order with edge frequencies 6Hz,12Hz ($\alpha-$band) and 25Hz, 45Hz ($\gamma-$band). Moreover, the instantaneous power in both bands $P_{\alpha,\gamma}$ illustrate well temporal alternations of power. A sliding window of duration $T_{\mathrm{segment}}/10$ (cf. section 2.1 for definition of T_{segment}) moves over the signal with time step $1/f_s$, in which the instantaneous power is computed to

$$P_{\alpha,\gamma}(t_j) = \frac{1}{N_w} \sum_{i=j}^{j+N_w} \mathrm{EEG}^2_{\alpha,\gamma}(t_i) \tag{8}$$

with discrete time points $t_j = j/f_s$, the integer number of time points in the sliding window $N_w = [T_{\mathrm{segment}} f_s]$ and the bandpass-filtered signal $\mathrm{EEG}_{\alpha,\gamma}$ in the $\alpha-$ and $\gamma-$band.

To illustrate further the alternating spectral power distribution in the course of time, we compute a trial-averaged time-frequency representation of the EEG spectral power. To this end, we computed the continuous wavelet transform

$$W_a(\tau) = \frac{1}{\sqrt{a}} \int_{-\infty}^{\infty} \mathrm{EEG}(t) \Psi \left(\frac{t-\tau}{a} \right) \, dt$$

by utilizing the Morlet mother wavelet

$$\Psi(x) = e^{-x^2/2}\cos(5x)$$

in the Python module *PyWavelet* (Lee et al. 2019). Here, τ is a time shift and a denotes the scale that is related to a pseudo-frequency (Mallat 1998) f by $a = f_c/(f\Delta t)$ with the center frequency f_c. In the implementation used it is $f_c = 0.8125$. This relates $W_a(\tau)$ to the time-frequency representation $W(f,\tau)$. Then the power spectral density about frequency f at time instance τ is $|W(f,\tau)|^2$.
For illustration, we have considered an EEG-signal segment of two periods, i.e. two states *eyes open* and *eyes closed*, as a single trial. Then the trial-averaged time-frequency spectral power is defined as

$$S(f,\tau) = \frac{1}{\text{trials}} \sum_{k=1}^{\text{trials}} |W_k(f,\tau)|^2 \ ,$$

where $W_k(f,\tau)$ is the continuous wavelet transform of EEG(t) in the $k-th$ 2 periods-segment. Figure 1(B) shows $S(f,\tau)$ for trials $= 25$.

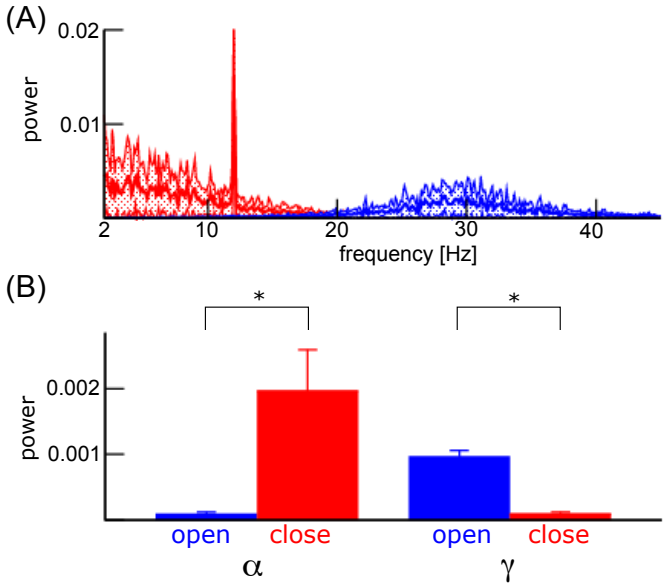

Fig. 4 Power spectra of the EEG-signal in condition *eyes open* (blue) and *eyes closed* (red). (A) The power averaged over $P = 20$ intervals (bold line) between maxima and minima at vertical standard deviation distance (shaded area). (B) Power statistics in the $\alpha-$ and $\gamma-$band in the two conditions, $p < 0.05$.

3 Results

We assume that opening eyes increases the ARAS activity through visual attention and elevates the level of brain excitability. To mimic this in our model, the arousal state function $e(t)$ (Eq. (1)) reaches its maximum during states of arousal and thus intrinsic noise in both cortical layer I-III and V+VI are maximum as well. Figure 3(A) illustrates the arousal state function alternating between the states *eyes open* and *eyes closed* implying alternating noise levels betwen two different ARAS mediated arousal states. The resulting EEG mirrors these fluctuations: the time series exhibits alternations between high-frequency, low-amplitude oscillations at *eyes open* conditions and low-frequency high-amplitude oscillations at *eyes closed* state (Fig. 3(B)). These alternating states exhibit strong $\gamma-$ and $\alpha-$activity (Fig. 3(C)). Taken together, switches between *eyes open* and *eyes closed*, mediated by changes in the arousal state function amplitude, lead to anti-correlated switches between strong $\gamma-$ and α-activity, cf. Fig. 3(D). These results are in good agreement with experimental observations in the visual cortex, cf. Fig. 1.

A closer look at the power spectral density in both conditions clearly reveals that *open eyes* induces primarily $\gamma-$rhythms and *closed eyes* induces a strong $\alpha-$rhythm (Fig. 4(A)). This switch of power was further found to be statistically significant, see Fig. 4(B). These results suggest that changes in arousal state lead to alternation in the dominant peak frequency expressed whithin cortical populations through an interaction with the thalamocortical feedback loop.

To understand the underlying dynamics, we have computed the equilibria and their stability, cf. section 2.3 and Fig. 5. For low microscopic noise variances D_e^{ic} - characterizing the minimal arousal state - we observe bi-stability in the intracortical model with a top stable node, center saddle node and bottom stable focus (Fig. 5(A)). Increasing the microscopic noise variance, this bi-stability vanishes through a saddle-node bifurcation and a single bottom stable focus remains. Due to the presence of additive noise, this state exhibits quasi-cycles that are observed as a γ-peak in the signal's power spectrum. This noise-induced transition is a signature of coherence resonance. Taken together, this analysis reveals that opening eyes (that is modelled by maximizing the arousal state function e) induces coherence resonance in the γ-frequency band and closing eyes stabilizes the intracortical dynamics about a stable node.
Concurrently, the cortico-thalamic feedback network exhibits a shift away from an oscillatory instability threshold towards a more stable focus equilibrium as microscopic noise level D_o^{ct} is increased (Fig. 5(B)). Increasing the noise stabilizes the dynamics by pushing the fixed point further from the limit cycle regime, suppressing the amplitude of the quasi-cycle which is responsible of observed cortico-thalamic fluctuations. The

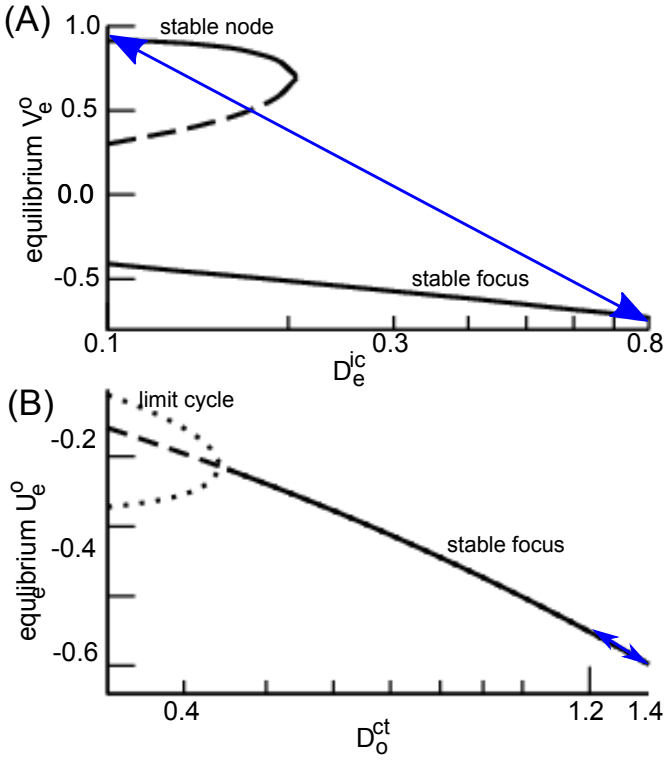

Fig. 5 Bifurcation diagrams of both cortical and thalamocortical modules. (A) In the intracortical model (5) the system transitions from a stable node equilibrium in the top state at low noise variance $D_e^{\rm ic}$ to a stable focus equilibrium at high noise variance with a characteristic frequency in the γ-band, i.e. the system exhibits coherence resonance. (B) In the cortico-thalamic model (6) the noise variance $D_o^{\rm ct}$ is chosen that the system evolves about a stable focus equilibrium (in the $\alpha-$frequency band) below an oscillatory instability point. Increasing $D_o^{\rm ct}$ moves the system away from the instability point and diminishes the quasi-cycle amplitude. The arousal state function $e(t)$, cf. Eq. (1), moves the system back and forth along the blue-colored double arrow in time. Solid and dashed lines denote stable (unstable) equilibria, the dotted lines in (B) denote the maximum and minimum values of a nonlinear limit cycle.

characteristic frequency of this quasi-cycle is in the $\alpha-$frequency band. Hence, opening the eyes quenches and suppresses the cortico-thalamic feedback oscillations by increasing microscopic noise, while closing eyes amplifies oscillatory activity through a reduction in ARAS-mediated inputs, i.e. reduction of microscopic noise, reminiscent of experimental observations with the $\alpha-$rhythm.

4 Discussion

Arousal is a brain mechanism that acts like an activation gate to recruit neural populations and determines their excitability in a task-dependent way. The Ascending Reticular Arousal System, involving the brain stem and related structures, is one of the main driver of arousal, projecting to various brain areas and impacting their dynamics. One of the most salient dynamical hallmark of arousal are shifts in oscillatory neural activity observed in occipital cortical areas with increased visual stimuli, notably when animals open and/or close their eyes. The α-rhythm, one of the most robust biomarkers of brain states observed with EEG, dominates in states of low arousal. Upon increases in arousal, the α-rhythm is suppressed and replaced by other, typically faster and more local oscillations, such as the γ-rhythm.

We propose that alternations between those dominant oscillatory modes are controlled by ARAS in an arousal-dependent way. While the mechanisms remain unclear, insight can be gained by observing how ARAS-mediated inputs engage and interfere with the neural circuitry responsible of these anti-correlated rhythms. Whereas α-activity likely has a thalamocortical origin, specifically between thalamic regions and layers IV-VI of the cortex, the γ-rhythm has been shown to originate from superficial cortical areas, namely layers I-III.

To better understand these oscillatory transitions and the role played by the ARAS, we developed and analyzed a thalamocortical feedback model coupled with a superficial cortical network model that exhibits anti-correlated α and γ oscillations. Specifically, our model shows that arousal-mediated inputs - which take the form of uncorrelated noise mimicking afferent spiking activity - provoked alternation in dominant oscillations, enabling transitions between slow thalamocortical oscillations and fast cortical oscillations. Mathematical analysis revealed that $\alpha-$activity is a noise-driven quasi-cycle which is suppressed by noisy inputs and replaced by fast, quasi-cycle like responses in superficial layers through the mechanism of coherence resonance. Taken together, these results are in good agreement with experimental data observed in ECog-data in these frequency bands during arousal fluctuations (Geller et al. 2014).

Our computational and mathematical results shed a new light on the mechanism underlying the suppression of EEG slow wave activity observed during visual attention and overt behavior, a phenomenon referred to as Event Related Desynchronization (ERD). Such desynchronization that preferentially targets the α-band during movement and/or sensory stimulation, has been historically linked to an elevated activation state of the cortex through a significant suppression of slow frequency spectral power (Steriade et al. 1991a). The opposite effect, called Event Related Synchronization (ERS), in which spectral power increases within the same bands during withdrawal, has been linked in contrast to a disengagement of cortical networks and thus

interpreted as a form of functional inhibition (Klimesch, Sauseng, and Hanslmayr 2007; Pfurtscheller 2001). Our results show that ARAS-mediated inputs can engage and interfere with cortical and subcortical networks to mediate such transitions spontaneously - and supports the hypothesis by which the suppression of α-power reflects enhanced activation of cortical activity. Furthermore, our results suggest that focal activation of task-relevant circuits would support spatially localized oscillatory transitions, such as those observed in experiments (Pfurtscheller and Silva 1999) and computational simulations (Griffith, McIntosh, and Lefebvre 2021).

4.1 Insights about the mechanisms of $\gamma-$ and α-rhythms generation

In our model, this switch involves a coherence resonance-like mechanism in the supragranular layers of the occipital cortex as $\gamma-$rhythm generator. The neural noise that induces this rhythm originates from the brain stem or, more generally, from the ARAS (cf. Fig. 2). Previous experimental (Hakim, Shamardani, and Adesnik 2018; Niell and Stryker 2010; Pisarchik et al. 2019) and theoretical (Tchumatchenko and Clopath 2014) studies seem to confirm this theoretical finding. In more general terms, this affirms the hypothesis that intrinsic neural noise affects the information processing heavily in the brain (Pertermann et al. 2019; Solanka, van Rossum, and Nolan 2015).
Our study proposes that the dominant $\alpha-$power observed in human subjects with closed eyes or, equivalently low arousal, represents a quasi-cycle generated by thalamocortical feedback. This cycle has a large magnitude for low arousal (eyes closed) and vanishes for high arousal (eyes open). This is consistent with an experimental study on the impact of arousal on the power and frequency of occipital $\alpha-$activity (Cantero et al. 1999).
The proposed model includes two distinct sub-models, which are different in their network topology and underlying dynamics. This distinction between the cortico-thalamic feedback loop and an intra-cortical network generating slow-large amplitude and fast-low amplitude rhythms is in full line with experimental findings (Bastos et al. 2014).

4.2 Limitations

In addition to switches in $\gamma-$ and $\alpha-$ in the occipital cortex, several previous experimental studies have highlighted changes in other frequency bands in various brain areas due to changes in arousal level and/or opening and closing eyes (Barry and De Blasio 2017; Geller et al. 2014). Parietal areas show switches between $\alpha-$ and $\gamma-$rhythms similar to our results, whereas frontal areas do not show such bimodality. As such, our model focuses on the occipital areas solicited by visual arousal. Future work will determine which model elements are thought to differ across brain areas and thus identify brain area-specific mechanisms. However, we mention that our cortico- thalamic feedback model already permits to describe the propofol- induced induction of $\alpha-$ activity observed in frontal regions under general anaesthesia (Hutt et al. 2018). This reinforces the relevance of our model as it permits to describe the generation of α-activity in two different experimental conditions by the same underlying mechanism: the decrease of ARAS activity.
Apart from the focus on a specific brain area, the single neuron dynamics and the network topology in our model are oversimplified to the cost of important neurophysiolical details. The cortico-thalamic model neurons employ a Poisson firing statistics and the intracortical neurons a traditional static McCullogh-Pitts firing mechanism. Moreover, the networks are assumed being homogeneous that is an obvious simplification. We have chosen such simple properties in order to discover a fundamental mechanism underlying the brain dynamics. This line of argumentation follows the principle research approach that a real-existing mechanism observed in simple but still reasonable neural models remains valid in biologically more realistic models. Of course, future work will have to extend the presented models to verify this research approach. However, the coherence resonance and dynamic transition mechanism proposed in this work has been found in previous biologically more realistic models already.

5 Declarations

Funding

Not applicable

Conflicts of interest/Competing interests

The authors declare that they have no conflict of interest or any competing interests.

Availability of data and material

Not applicable

Code availability

The implementation code of the model will be made available for request.

Authors' contributions

AH has conceived the work and both authors have written the manuscript.

Acknowledgements JL thanks National Research Council of Canada Grant RGPIN-2017-06662 and Canadian Institute for Health Research Grant NO PJT-156164 for funding.

References

Adrian, E.D. and B.H.C. Matthews (1935). The Berger rhythm: potential changes from the occipital lobes in man. *Brain* 57.4, p. 355.

Amari, S. (1977). Dynamics of Pattern Formation in Lateral-Inhibition Type Neural Fields. *Biol. Cybernetics* 27, pp. 77–87.

Barry, R.J. and F.M. De Blasio (2017). EEG differences between eyes-closed and eyes-open resting remain in healthy ageing. *Biol. Psychol.* 129, pp. 293–304. DOI: 10.1016/j.biopsycho.2017.09.010.

Bastos, A.M. et al. (2014). Simultaneous Recordings from the Primary Visual Cortex and Lateral Geniculate Nucleus Reveal Rhythmic Interactions and a Cortical Source for Gamma-Band Oscillations. *J. Neurosci.* 34.22, pp. 7639–7644. DOI: 10.1523/JNEUROSCI.4216-13.2014.

Berger, H. (1935). Über das Elektroenzephalogram des Menschen. 10. Mitteilung. *Archiv fü Psychiatrie* 103, p. 444.

Bollimunta, A. et al. (2008). Neuronal Mechanisms of Cortical Alpha Oscillations in Awake-Behaving Macaques. *J. Neurosci.* 28.40, pp. 9976–9988. DOI: 10.1523/JNEUROSCI.2699-08.2008.

Bollimunta, A. et al. (2011). Neuronal Mechanisms and Attentional Modulation of Corticothalamic Alpha Oscillations. *J. Neurosci.* 31.13, pp. 4935–4943. DOI: 10.1523/JNEUROSCI.5580-10.2011.

Brown, E.N., R.L. Lydic, and N.D. Schiff (2010). General anesthesia, sleep, and coma. *N Engl J Med* 363, pp. 2638–2650.

Brown, R.E. et al. (2012). Control of sleep and wakefulness. *Physiol. Rev.* 92.3, pp. 1087–1187. DOI: 10.1152/physrev.00032.2011.

Buckwar, E. and R. Winkler (2007). Multi-Step Maruyama Methods for Stochastic Delay Differential Equations. *Stoch. Anal. Appl.* 25.5, pp. 933–959.

Cantero, J.L. et al. (1999). Spectral Structure and Brain Mapping of Human Alpha Activities in Different Arousal States. *Neuropsychobiol.* 39, pp. 110–116. DOI: 10.1159/000026569.

Coull, J.T. (201998). Neural correlates of attention and arousal: insights from electrophysiology, functional neuroimaging and psychopharmacology. *Prog. Neurobiol.* 55.4, pp. 343–361. DOI: 10.1016/s0301-0082(98)00011-2.

Edlow, B.L. et al. (2012). Neuroanatomic Connectivity of the Human Ascending Arousal System Critical to Consciousness and Its Disorders. *J. Neuropathol. Exp. Neurol.* 71.6, pp. 531–546. DOI: 10.1097/NEN.0b013e3182588293.

Franks, N.P. (2008). General anesthesia: from molecular targets to neuronal pathways of sleep and arousal. *Nat.Rev.Neurosc.* 9, pp. 370–386. DOI: 10.1038/nrn2372.

Fries, P. et al. (2001). Modulation of oscillatory neuronal synchronization by selective visual attention. *Science* 291, pp. 1560–1563.

Fuller, P. et al. (2011). Reassessment of the structural basis of the ascending arousal system. *J. Comput. Neurol.* 519.5, pp. 933–956. DOI: 10.1002/cne.22559.

Gang, H. et al. (1993). Stochastic resonance without external periodic force. *Phys. Rev. Lett.* 71, pp. 807–810.

Geller, A.S. et al. (2014). Eye closure causes widespread low-frequency power increase and focal gamma attenuation in the human electrocorticogram. *Clin. Neurophysiol.* 125.9, pp. 1764–1773. DOI: 10.1016/j.clinph.2014.01.021.

Griffith, J., A.R. McIntosh, and J. Lefebvre (2021). A connectome-based, corticothalamic model of state- and stimulation-dependent modulation of rhythmic neural activity and connectivity. *Front. Comp. Neurosci.* accepted. DOI: doi:10.3389/fncom.2020.575143.

Hakim, R., K. Shamardani, and H. Adesnik (2018). A neural circuit for gamma-band coherence across the retinotopic map in mouse visual cortex. *eLife* 7, e28569. DOI: 10.7554/eLife.28569.

Halgren, M. et al. (2019). The generation and propagation of the human alpha rhythm. *Proc. Natl. Acad. Sci. USA* 116.47, pp. 23772–23782. DOI: 10.1073/pnas.1913092116.

Hashemi, M., A. Hutt, and J. Sleigh (2015). How the cortico-thalamic feedback affects the EEG power spectrum over frontal and occipital regions during propofol-induced anaesthetic sedation. *J. Comput. Neurosci.* 39.1, p. 155.

Herrmann, C. S. et al. (2016). Shaping Intrinsic Neural Oscillations with Periodic Stimulation. *J. Neurosci.* 36.19, pp. 5328–5339.

Hughes, S.W. and V. Crunelli (2005). Thalamic Mechanisms of EEG Alpha Rhythms and Their Pathological Implications. *The Neuroscientist* 11.4, pp. 357–372.

Hutt, A., ed. (2011). *Sleep and Anesthesia: Neural Correlates in Theory and Experiment*. Springer Series in Computational Neuroscience 15. Springer, New York.

— (2013). The anaesthetic propofol shifts the frequency of maximum spectral power in EEG during general anaesthesia: analytical insights from a linear model. *Front. Comp. Neurosci.* 7, p. 2.

— (2019). Cortico-Thalamic Circuit Model for Bottom-Up and Top-Down Mechanisms in General Anesthesia Involving the Reticular Activating System. *Arch. Neurosci.* accepted. DOI: 10.5812/ans.95498.

Hutt, A. and L. Buhry (2014). Study of GABAergic extra-synaptic tonic inhibition in single neurons and neural populations by traversing neural scales: application to propofol-induced anaesthesia. *J. Comput. Neurosci.* 37.3, pp. 417–437.

Hutt, A., A. Mierau, and J. Lefebvre (2016). Dynamic Control of Synchronous Activity in Networks of Spiking Neurons. *PLoS One* 11.9, e0161488. DOI: 10.1371/journal.pone.0161488.

Hutt, A. et al. (2018). Suppression of underlying neuronal fluctuations mediates EEG slowing during general anaesthesia. *Neuroimage* 179, pp. 414–428.

Hutt, A. et al. (2020). Phase coherence induced by additive Gaussian and non-Gaussian noise in excitable networks with application to burst suppression-like brain signals. *Front. Appl. Math. Stat.* 5, p. 69. DOI: 10.3389/fams.2019.00069.

Kim, T. et al. (2015). Cortically projecting basal forebrain parvalbumin neurons regulate cortical gamma band oscillations. *Proceed. Natl. Acad. Sci.* 112.11, pp. 3535–3540. DOI: 10.1073/pnas.1413625112.

Klimesch, W., P. Sauseng, and S. Hanslmayr (2007). EEG alpha oscillations: the inhibition-timing hypothesis. *Brain Res. Rev.* 53.1, pp. 63–88. DOI: 10.1016/j.brainresrev.2006.06.003.

Koval'zon, V.M. (2013). The role of histaminergic system of the brain in the regulation of sleep-wakefulness cycle. *Hum Physiol* 39.6, pp. 574–583. DOI: 10.1134/S0362119713060078.

— (2016). Ascending reticular activating system of the brain. *Transl. Neurosci. Clin.* 2.4, pp. 275–285. DOI: 10.18679/CN11-6030/R.2016.034.

Lakatos, P. et al. (2004). Attention and arousal related modulation of spontaneous gamma-activity in the auditory cortex of the cat. *Brain Res. Cogn. Brain Res.* 19.1, pp. 1–9. DOI: 10.1016/j.cogbrainres.2003.10.023.

Lee, G.R. et al. (2019). PyWavelets: A Python package for wavelet analysis. *J. Open Source Software* 4.36, p. 1237. DOI: 10.21105/joss.01237.

Lee, K. et al. (2003). Synchronous Gamma activity: a review and contribution to an integrative neuroscience model of schizophrenia. *Brain Res. Rev.* 41, pp. 57–78.

Lefebvre, J., A. Hutt, and F. Frohlich (2017). Stochastic Resonance Mediates the State-Dependent Effect of Periodic Stimulation on Cortical Alpha Oscillations. *eLife* 6, e32054.

Lefebvre, J. et al. (2015). Stimulus statistics shape oscillations in nonlinear recurrent neural networks. *J. Neurosci.* 35.7, pp. 2895–2903.

Longtin, A. (1997). Autonomous stochastic resonance in bursting neurons. *Phys. Rev. E* 55, pp. 868–876.

Mallat, S. (1998). *A wavelet tour of signal processing: the sparse way*. 3rd. Academic Press, London.

McNally, J.M. et al. (2020). Optogenetic manipulation of an ascending arousal system tunes cortical broadband gamma power and reveals functional deficits relevant to schizophrenia. *Mol Psychiatry* in press. DOI: 10.1038/s41380-020-0840-3.

Moruzzi, G. and H.W. Magoun (1949). Brainstem reticular formation and activiation of the EEG. *Electroencephalogr. Clin. Neurophysiol.* 1, pp. 455–473.

Munk, M.H. et al. (1996). Role of reticular activation in the modulation of intracortical synchronization. *Science* 272, pp. 271–274.

Niell, C.M. and M.P. Stryker (2010). Modulation of visual responses by behavioral state in mouse visual cortex. *Neuron* 65.4, pp. 472–479.

Pertermann, M. et al. (2019). The Modulation of Neural Noise Underlies the Effectiveness of Methylphenidate Treatment in Attention-Deficit/Hyperactivity Disorder. *Biol. Psychiatry* 4 (8), pp. 743–750. DOI: 10.1016/j.bpsc.2019.03.011.

Pfurtscheller, G. (2001). Functional brain imaging based on ERD/ERS. *Vision Res.* 41.10-11, pp. 1257–1260. DOI: 10.1016/s0042-6989(00)00235-2.

Pfurtscheller, G. and F.H. Lopes da Silva (1999). Event-related EEG/MEG synchronization and desynchronization: basic principles. *Clin Neurophysiol.* 110.11, pp. 1842–1857.

Pikovsky, A.S. and J. Kurths (1997). Coherence Resonance in a Noise-Driven Excitable System. *Phys. Rev. Lett.* 78, pp. 775–778.

Pisarchik, A.N. et al. (2019). Coherent resonance in the distributed cortical network during sensory informa-

tion processing. *Sci. Rep.* 9, p. 18325. DOI: 10.1038/s41598-019-54577-1.

Quinkert, A.W. et al. (2011). Quantitative descriptions of generalized arousal, an elementary function of the vertebrate brain. *Proc. Natl. Acad. Sci. USA* 108, pp. 15617–15623.

Rich, S. et al. (2020). Neurostimulation stabilizes spiking neural networks by disrupting seizure-like oscillatory transitions. *Sci. Rep.* 10, p. 15408. DOI: 10.1038/s41598-020-72335-6.

Richter, C., I.G. Woods, and A.G. Schier (2014). Neuropeptidergic control of sleep and wakefulness. *Annu. Rev. Neurosci.* 37, pp. 503–531. DOI: 10.1146/annurev-neuro-062111-150447.

Schiff, N.D. (2008). Central thalamic contributions to arousal regulation and neurological disorders of consciousness. *Ann. NY. Acad. Sci.* 1129, pp. 105–118.

Sleigh, J.W. et al. (2011). "Modelling Sleep and General Anaesthesia". In: *Sleep and Anesthesia: Neural correlates in Theory and Experiment*. Ed. by A. Hutt. Springer, New York, pp. 21–41.

Solanka, L., M.C.W. van Rossum, and M.F. Nolan (2015). Noise promotes independent control of gamma oscillations and grid firing within recurrent attractor networks. *eLife* 4, e06444. DOI: 10.7554/eLife.06444.

Steriade, M. (1996). Arousal–Revisiting the Reticular Activating System. *Science* 272, p. 225.

Steriade, M., D.A. McCormick, and T.J. Sejnowski (1993). Thalamocortical Oscillations in the Sleeping and Aroused Brain. *Science* 262, pp. 679–685.

Steriade, M. et al. (1991a). Basic mechanisms of cerebral rhythmic activities. *Electroencephalogr. Clin. Neurophysiol.* 76, pp. 481–508.

Steriade, M. et al. (1991b). Fast oscillations (20–40 Hz) in thalamocortical systems and their potentiation by mesopontine cholinergic nuclei in the cat. *Proc. Natl. Acad. Sci. USA* 88, pp. 4396–4400.

Tchumatchenko, T. and C. Clopath (2014). Oscillations emerging from noise-driven steady state in networks with electrical synapses and subthreshold resonance. *Nat. Commun.* 5, p. 5512. DOI: 10.1038/ncomms6512.

Thut, G. et al. (2006). α-Band Electroencephalographic Activity over Occipital Cortex Indexes Visuospatial Attention Bias and Predicts Visual Target Detection. *J. Neurosci.* 26.37, pp. 9494–9502.

Vijayan, S. and N.J. Kopell (2012). Thalamic model of awake alpha oscillations and implications for stimulus processing. *Proc. Natl. Acad. Sci. USA* 109.45, pp. 18553–18558. DOI: 10.1073/pnas.1215385109.

Wilson, H.R. and J.D. Cowan (1972). Excitatory and inhibitory interactions in localized populations of model neurons. *Biophys. J.* 12, pp. 1–24.